Contents

Chapter 1

Chua's Equation was Proved to be Chaotic in Two Years, Lorenz Equation in Thirty Six Years

Bharathwaj Muthuswamy

Department of EECS, Milwaukee School of Engineering, USA

Contents

1. Introduction

In this chapter, we study what is probably one of the most important contributions to chaos theory, Leon O. Chua's namesake Chua's circuit. This circuit is considered a paradigm because it is a fact that Chua's circuit is the first chaotic system in which chaos was systematically derived,[Chua(1992)] physically confirmed[Matsumoto(1984)] and rigorously analyzed.[Chua et. al.(1986)] The purpose of this chapter is to explore the systematic realization and rigorous analysis of chaos in Chua's circuit. Nevertheless, in order to understand why these facts are important, we must turn to a brief history of chaos.[Alligood et. al.(1996)]

Chaos was actually observed by Henri Poincaré in the late 1800s while working on the three body problem in astronomy. It was also observed by Van der Pol in the late 1920s in the very first electronic oscillator. However, Edward N. Lorenz published the first paper[Lorenz(1963)] that exclusively addressed the main features[a] of a chaotic system - sensitivity to initial conditions, aperiodicity and boundedness of trajectories. His 1963 paper was related to work he initially did in 1961 at the Travelers Insurance Company Weather Center in Hartford, Connecticut. Lorenz was shown a 7-equation model of fluid convective motion. Lorenz simplified this model into a 3-equation system of nonlinear Ordinary Differential Equations (ODEs), shown in Eqs.(1) through (3).

$$\dot{x} = -\sigma x + \sigma y \tag{1}$$
$$\dot{y} = -xz + \rho x - y \tag{2}$$
$$\dot{z} = xy - \beta z \tag{3}$$

The dot notation has been used to indicate a derivative with respect to time and will be employed throughout this chapter. For $\sigma = 10, \beta = \frac{8}{3}$, Lorenz observed via computer simulations that the system behaved "chaotically" whenever ρ exceeded the approximate critical value of 24.74. A phase plot $(x(t), y(t), z(t))$

[a]We want to emphasize these features are not the definition of a chaotic system. To understand why no definition of chaos presently exists, please refer to.[Brown and Chua(1996)]

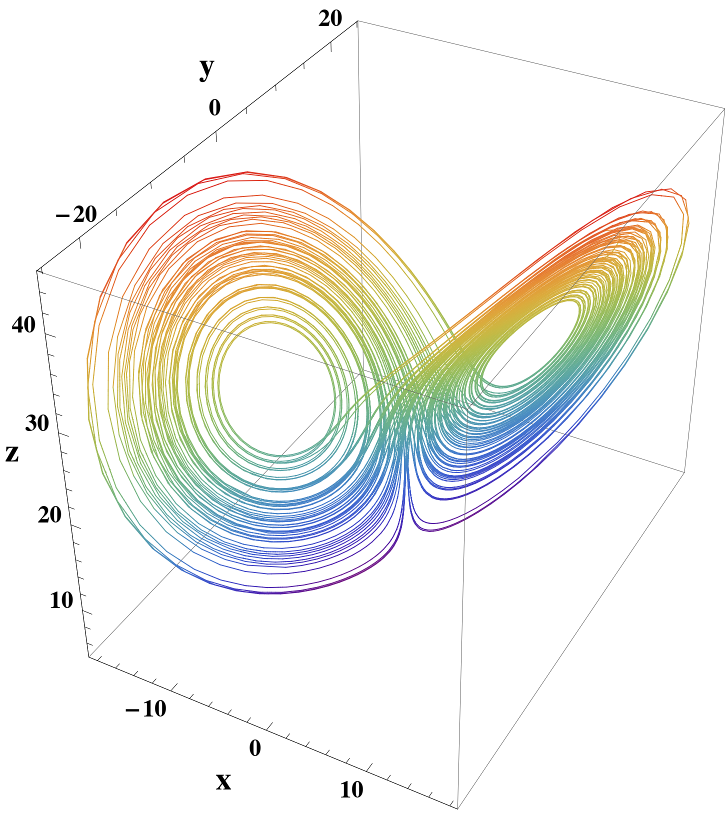

Fig. 1. The Lorenz butterfly. It is also called as a "chaotic attractor" because the underlying system exhibits chaotic behavior and nearby initial conditions are "attracted" into the butterfly. The attractor trajectory has been colored to highlight the unique shape in three dimensional space.

obtained from numerical simulation of Eqs.(1) through (3) has been plotted in Fig. 1. The system equations have been numerically simulated and rendered using Mathematica 8.[Mathematica(2011)] All calculations were also performed using Mathematica. The Mathematica source for this chapter can be found online at `http://myweb.msoe.edu/muthuswamy/MuthuswamyWSPC2011ChuaBook-OnlineFiles/`.

Although Lorenz's clever geometric arguments[Lorenz(1963)] implied that chaos in Eqs.(1) through (3) was not a mathematical anomaly, no one could reproduce chaos physically in the 1970s and early 1980s. Thus, in order to verify that steady-state chaotic behavior was not an artifact of computer simulations, there was a need for a physical chaotic system. One of the main reasons for the lack of a physical realization of early chaotic systems such as Lorenz and Rössler's equations[Rossler(1976)] was the presence of multiplier terms in the nonlinearities. These terms were hard to realize physically, especially electronically since the analog multiplier did not become a reliable electronic component[Chua(1992)] till the late 1980s.

The lack of a physical realization would change in 1983, twenty years after Lorenz's paper, when Leon O. Chua systematically derived Chua's circuit. Because of the systematic derivation, Chua's circuit utilized piecewise-linear nonlinearities as opposed to product terms. Hence physical realization of Chua's circuit and a rigorous proof of chaos would only take a total of two years.[Chua(1992)] In contrast the first electronic realization of Lorenz's system[Tokunaga et. al.(1989)] was done, interestingly enough, using piecewise linear approximations to the product terms in 1989. Rigorous proof of chaos in the Lorenz system[Tucker(1999)] would only be published in 1999, thirty six years after Lorenz's seminal work.

The rest of this chapter will study some of the most important properties of Chua's circuit. First we will systematically design and realize Chua's circuit.[Matsumoto(1984)] Next we will emphasize why a rigorous proof of chaos is necessary and outline the approach for proving rigorous existence of chaos in Chua's circuit. This

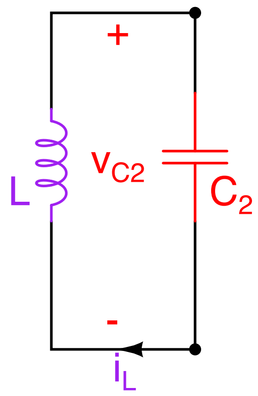

Fig. 2. The LC oscillator with the elements corresponding to different state variables highlighted in different color. We have two state variables, the current through inductor L given by $i_L(t)$ and the voltage across capacitor C_2 given by $v_{C2}(t)$. We will drop the explicit time reference since the independent variable in our differential equations is time.

section will serve as a "cookbook" for the reader in proving rigorous existence of chaos in piecewise-linear systems. We emphasize piecewise-linear systems because section 4 will provide a systematic tutorial on the Global Unfolding Theorem[Chua(1993)] by generalizing Chua's circuit to Chua's oscillator. This theorem will allow the reader to apply the rigorous proof of chaos from section 3 to a much larger class of piecewise-linear systems. The chapter will conclude with suggestions for further exploring chaos.

2. The Design and Realization of Chua's Circuit

Based on the previous section, a brief problem statement[Chua(1992)] is given below.

Design a physically realizable autonomous circuit exhibiting steady-state chaotic behavior.

We choose an autonomous chaotic circuit because this will eliminate the need for an external driving input such as a sinusoidal source. The requirement of an active circuit nonlinearity for chaos will be satisfied through operational amplifiers driven by DC sources (batteries).

Next we need to satisfy the Poincaré-Bendixson theorem, namely, we require at least three state variables for a continuous time autonomous dynamical system to be chaotic. In the case of electronic circuits, a natural choice of state variables are current and voltage. The typical linear passive inductor-capacitor or LC circuit in Fig. 2 is thus a good starting point because this circuit gives us two out of three state variables - the current through the inductor and the voltage across the capacitor.

In order to obtain the final state, we will choose a linear passive capacitor, since the range of values for a physical capacitor is quite a lot more when compared to physical inductors. Since we have all three state variables, we will choose the nonlinear component as an active memoryless device. Hence we will need only more component to complete the circuit because we need to separate the two voltage state variables across the capacitors. A linear passive resistor is chosen as the final component and the topology of Chua's circuit is shown in Fig. 3.

Note that the equilibrium configuration of circuit is very simple and is shown in Fig. 4. If we now choose the active nonlinearity as shown in Fig. 5, we get three equilibrium points and hence we can obtain chaos via Shilnikov's theorem.[Chua et. al.(1986)]

Physical realization of the nonlinear resistor is usually done using operational amplifiers as shown in Fig. 6. Having designed the nonlinear function, Eqs.(4) through (6) are the dynamical equations describing Chua's

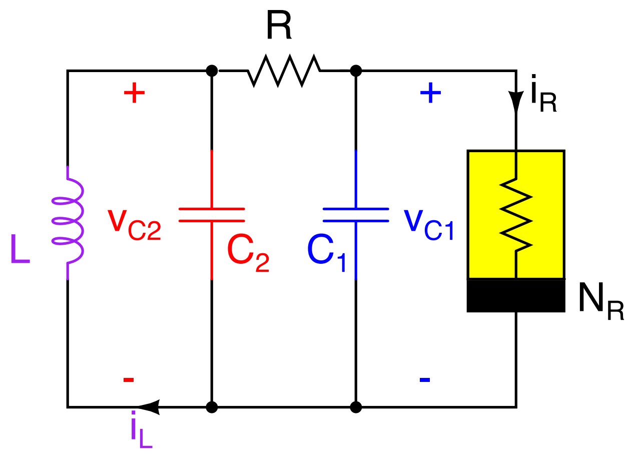

Fig. 3. Chua's circuit. The third state variable is the voltage v_{C1} across capacitor C_1. We have also added the linear passive resistor R and the nonlinear active resistor, N_R.

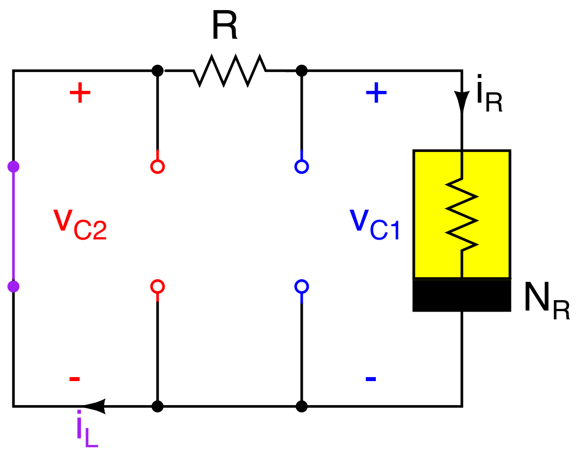

Fig. 4. Equilibrium or steady-state configuration of Chua's circuit. The dynamic elements have been replaced by their steady-state equivalents. The inductor is modeled by a short circuit and the capacitors are modeled by open-circuits.

circuit in Fig. 6.

$$C_1 \frac{dv_{C1}}{dt} = \frac{v_{C2} - v_{C1}}{R} - g(v_{C1}) \tag{4}$$

$$C_2 \frac{dv_{C2}}{dt} = \frac{v_{C1} - v_{C2}}{R} + i_L \tag{5}$$

$$L \frac{di_L}{dt} = -v_{C2} \tag{6}$$

Equation (7) defines a five-segment piecewise-linear function $g(\cdot)$ from Fig. 5. Only the inner three segments in Fig. 5 are relevant for obtaining chaos in Chua's circuit. The outer two segments, or their nonlinear counterparts, will always be exhibited in any physical realization of the nonlinear resistor (also known in literature as the Chua diode). The outer two segments are a consequence of the law of conservation of energy. They play no role, however, in the state space region covered by Chua's attractor.

$$g(v_R) = G_b v_R + \frac{1}{2}(G_a - G_b)\left(|v_R + B_p| - |v_R - B_p|\right) \tag{7}$$

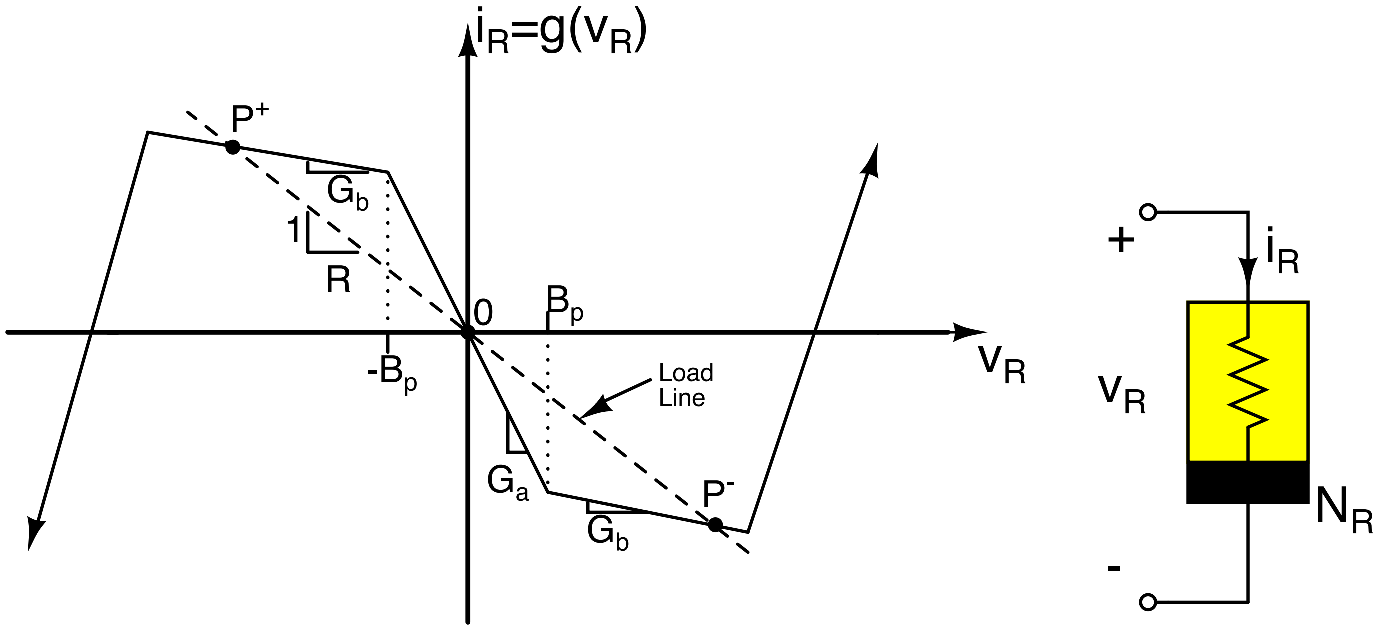

Fig. 5. The five segment piecewise-linear characteristic has three segments exclusively in the second and fourth quadrants. These correspond to the active region of the nonlinear resistor. In order to be physically realizable, notice that the nonlinear function eventually enters the first and third quadrants. Thus the nonlinear resistor is eventually passive. The linear resistor R has been plotted as a load and for particular values of R notice that we get three equilibrium points $P^{+}, 0, P^{-}$.

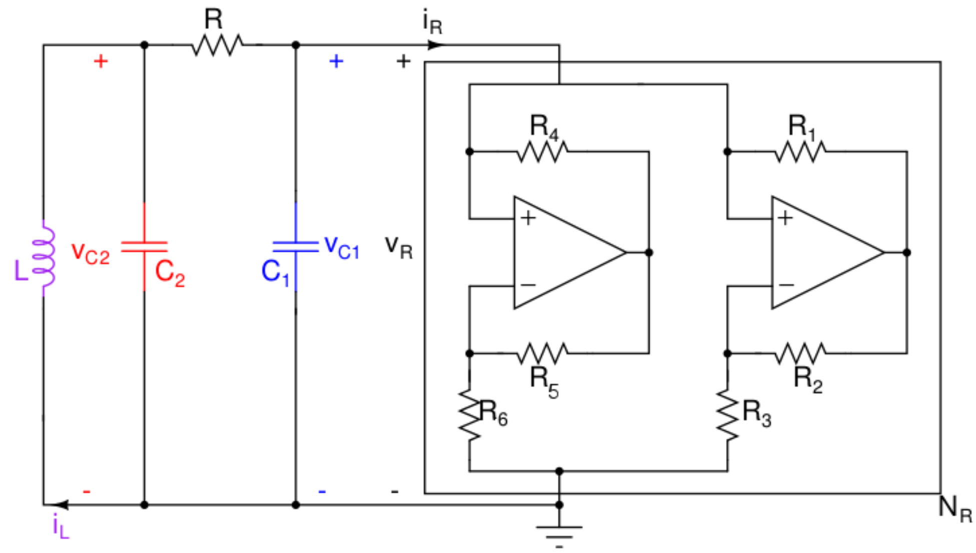

Fig. 6. Physical realization of Chua's circuit including the nonlinear resistor N_R. Parameter values[Matsumoto et. al.(1985)] are $L = 7.14\ mH, C_2 = 50\ nF, C_1 = 5.56\ nF, R = 1428\ \Omega$. Parameter values for the nonlinear resistor N_R[Kennedy(1992)] are $R_1 = R_2 = 220\ \Omega, R_3 = 2.0\ k\Omega, R_4 = R_5 = 22\ k\Omega, R_6 = 3.3\ k\Omega, B_p = 1\ V$. These values for the N_R realization lead to $G_a = \frac{-1}{R_3} - \frac{1}{R_6}$ (since $R_1 = R_2$), $G_b = \frac{-1}{R_3} + \frac{1}{R_4}$ (since $R_4 = R_5$). AD712 or equivalent operational amplifiers can be used, power supply for the op-amps are $\pm 9\ V$. The op-amp power supplies have been omitted for clarity. There are a variety of other ways to realize N_R, such as cross-coupled[O'Donoghue et. al. (2005)] inverters. Also the inductor and capacitor values were chosen to match Matsumoto's original[Matsumoto et. al.(1985)] paper. More realistic values[Kennedy(1992)] are $L = 18\ mH, C_2 = 100\ nF, C_1 = 10\ nF$.

Usually Eqs.(4) through (7) are scaled to be dimensionless via the following substitutions.

$$x \triangleq v_{C1}/B_p \qquad y \triangleq v_{C2}/B_p \qquad z \triangleq i_L R/B_p, \tag{8}$$

$$\tau \triangleq t/(RC_2) \qquad a \triangleq G_a R \approx \frac{-8}{7} \qquad b \triangleq G_b R \approx \frac{-5}{7}, \tag{9}$$

$$\alpha \triangleq C_2/C_1 \approx 9 \qquad \beta \triangleq C_2 R^2/L \approx 14\frac{2}{7} \tag{10}$$

Equations (11) through (14) are the dimensionless form of Chua's equation.

$$\dot{x} = \alpha(y - x - f(x)) \tag{11}$$

$$\dot{y} = x - y + z \tag{12}$$

$$\dot{z} = -\beta y \tag{13}$$

$$f(x) = bx + \frac{1}{2}(a - b)\left(|x + 1| - |x - 1|\right) \tag{14}$$

One further simplification for analysis is obtained by Eq.(15) from Eq.(14).

$$h(x) \triangleq x + f(x) = m_1 x + \frac{1}{2}(m_0 - m_1)(|x + 1| - |x - 1|) \tag{15}$$

Hence $m_0 = a + 1, m_1 = b + 1$. Thus the dimensionless form that will be used for a rigorous proof of chaos is given by Eqs.(16) through (19).

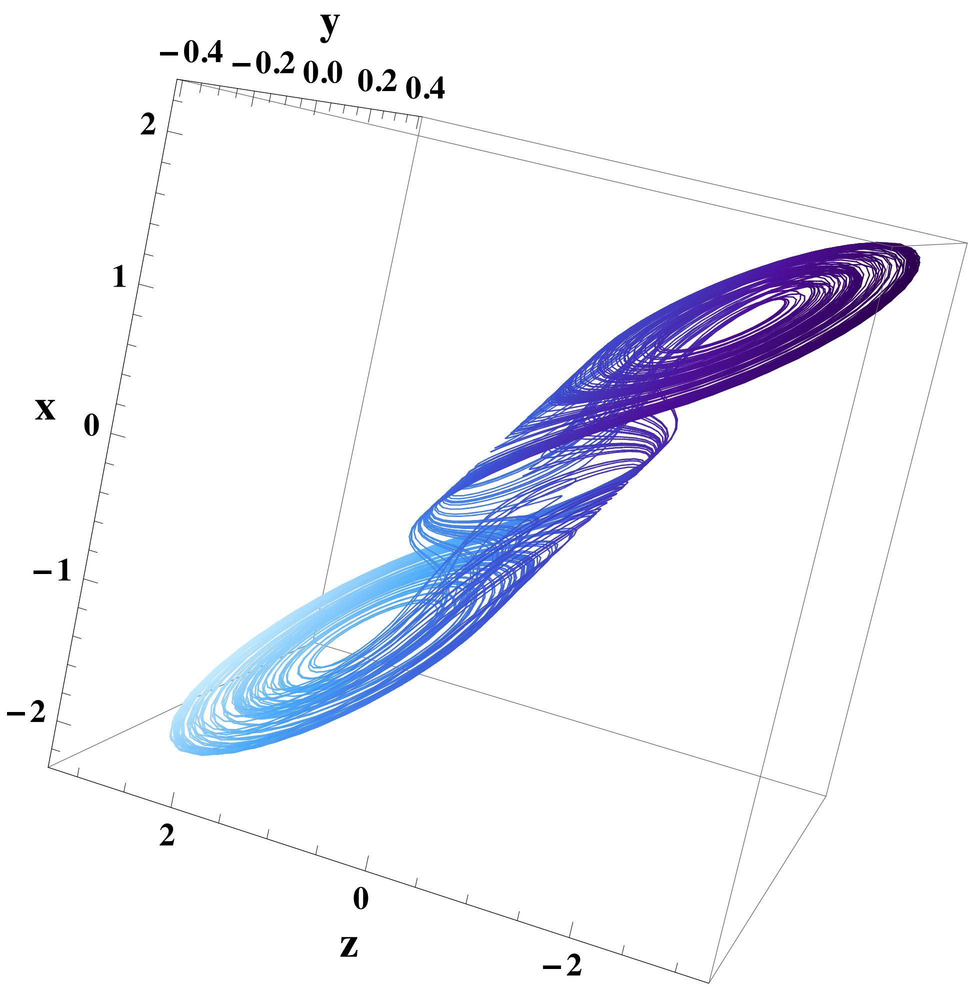

Fig. 7. The Double-Scroll Chua's attractor. Recall that Chua's circuit has three equilibrium points: $(P^+, 0, P^-)$. It turns out that the chaotic trajectory "wraps around" one of the outer equilibrium points (P^+, P^-) and then moves through the equilibrium point at the origin, to the other equilibrium point.

$$\dot{x} = \alpha(y - h(x)) \tag{16}$$

$$\dot{y} = x - y + z \tag{17}$$

$$\dot{z} = -\beta y \tag{18}$$

$$h(x) = m_1 x + \frac{1}{2}(m_0 - m_1)(|x+1| - |x-1|) \tag{19}$$

We will interchangeably use the words "Chua's circuit" and "Chua's system" to refer to Eqs.(16) through (19) from now on. From the parameter values in Fig. 6 we obtain $\{\alpha, \beta, m_0, m_1\} = \{9, 14\frac{2}{7}, -1/7, 2/7\}$.[Chua et. al.(1986)] The classic Double-Scroll Chua's attractor obtained with these parameter values is shown in Fig. 7.

An useful quantity (or measure) for a chaotic attractor is the dimension. We are familiar with the concept of a dimension for everyday objects : a solid sphere is three dimensional, the surface of a sphere is two dimensional etc. In the case of chaotic attractors, many definitions of dimension exist, we will examine the Lyapunov dimension.[Matsumoto et. al.(1985)] We can actually predict the range of the Lyapunov dimension without any computation. Figure 7 seems to imply that the chaotic attractor is three dimensional. However this attractor is not a solid object, it is more a "sheet-like" structure. So, is the dimension less than two? The answer is no because of the Poincaré-Bendixson theorem. Can the dimension be greater than three? The answer again is no because the system of equations for Chua's circuit is three dimensional[b]. Thus intuitively the Lyapunov dimension of the Double-Scroll must be between two and three. It turns out that the Lyapunov dimension of the Double-Scroll is approximately 2.13.[Matsumoto et. al.(1985)]

We conclude this section by discussing a subtle but very important concept that is often misunderstood : Chua's circuit is not an analog computer.

2.1. *Analog Computer Emulation of an ODE is not a Physical Circuit*

A common misconception is to equate an "analog computer" emulation of a system of ODEs to a physical circuit. The reasoning employed is that analog computers are made of physical circuit elements like op-amps, resistors, capacitors and inductors. However, this reasoning can be understood as erroneous by considering this fact : digital computers are also made of circuit elements. Yet no one calls a digital computer emulation of a system of ODEs as a physical circuit!

The importance of this concept can be further understood by considering the mass-damper-spring system in Figure 8 and the two circuit realizations shown. One is the analog computer emulation and the other is the LRC realization. It should be immediately apparent that the analog computer is simply a "signal flow" graph and cannot account for physical characteristics of the mass-damper-spring. For instance, the position and velocity of the mass is simply represented by the voltages across the two capacitors. Also, the transfer of energy between the mass and spring cannot be interpreted from the analog computer. This is because energy requires us to have the product of force waveform and the velocity waveform[c]. This is unavailable in the analog computer emulation.

In contrast, the LRC circuit is the true electrical analog of the mass-damper-spring. This is easily seen by simply comparing the differential equations. For the mass-damper-spring, we have Eq.(20).

$$M\ddot{x} + D\dot{x} + Kx = 0 \tag{20}$$

For the LRC circuit, we have Eq.(21)

$$L_p\ddot{q} + R_p\dot{q} + \frac{1}{C_p}q = 0 \tag{21}$$

Comparing Eqs. (20) and (21), we can see that the mass has a one-to-one correspondence to the inductor, the dampener corresponds to the resistor and the spring corresponds to $\frac{1}{C_p}$. Also note that the position is analogous to charge and velocity to current. Thus the LRC circuit is the electrical physical realization of the mass-damper-spring system.

By the same argument as above, Chua's circuit in Fig. 6 is not an analog computer model but a physical realization of Eqs.(16) through (18).

In concluding this section, note that the op-amp circuit is an "analog computer" simulation of the mechanical system, where the word "analog" is used, by tradition, to mean "continuous time" or "not digital". This should should not be interpreted as an "analogy" of the mechanical mass-damper-spring system. Indeed, the word "analog computer" is just a non-technical jargon to mean any systematic collection of basic components, such as op amps, integrators, resistors, inductor, capacitors, etc., packed inside a compact cabinet, with externally accessible switches, and other extra features to allow one to quickly interconnect a continuous-time circuit such that its state equation is the desired one. Once can also observe the time evolution of the state variable dynamics via an oscilloscope, in real time. In this sense, the op amp circuit in Fig. 8 for simulating the mass-damper-spring mechanical system is just a "poor man's analog computer", tailored to simulate the state equations of only one physical system.

[b]In the case of four (or more) autonomous nonlinear ordinary differential equations, we could have hyper (or higher-dimensional) chaotic attractors.

[c]Scalar product of force and velocity gives instantaneous power. Time integral of instantaneous power gives work done or energy.

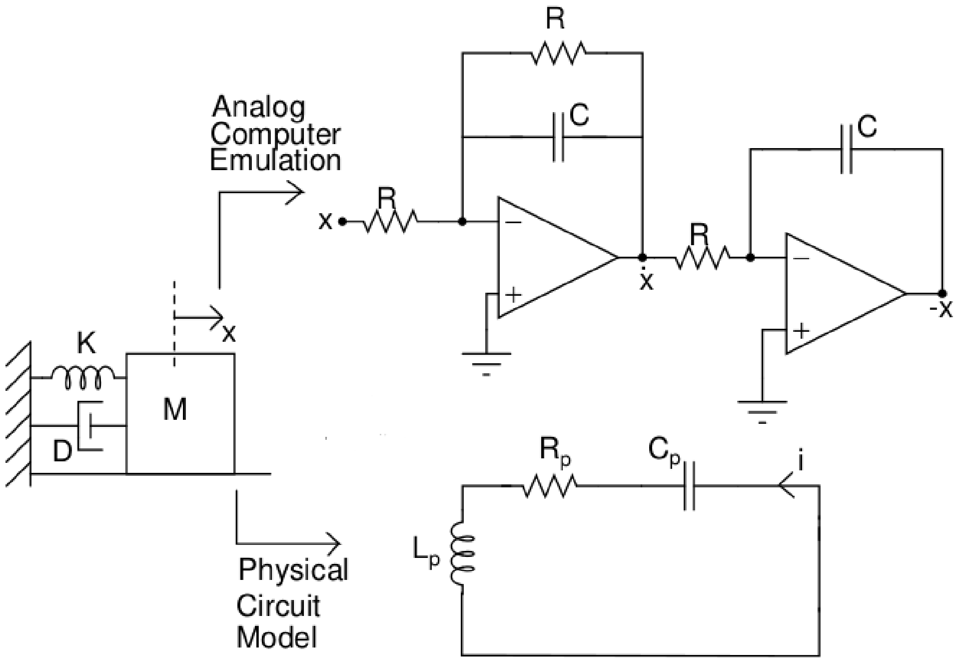

Fig. 8. The mass-damper-spring mechanical system and two electrical circuit versions. The voltages across the capacitor in the op-amp circuit correspond to the internal states of the mechanical system. However the analog computer version is an emulator whereas the LRC circuit is the actual physical electrical equivalent. Note that in deriving the analog computer, all mechanical parameters were assumed to have magnitude one. Moreover the analog circuit model actually requires one more inverting amplifier for producing x from $-x$.

3. The Need for a Rigorous Proof of Chaos

In the previous section, we examined the classic parameter values in Chua's circuit for obtaining Chua's attractor. If we can realize Chua's circuit and confirm chaos, why do we still need a rigorous proof? The answer is computer simulations have finite precision and experimental measurements have finite range for time or frequency. As a simple example, reconsider Chua's circuit with the parameter values $\{\alpha, \beta, m_0, m_1\} = \{10.75, 14\frac{2}{7}, -1/7, 2/7\}$. Note that we only changed the α value. A simulation of the system for four time intervals is shown in Fig. 9.

It is clear from Fig. 9 that we are observing chaos as a transient. If one were to consider only the first 30 time units , we would incorrectly conclude the system was exhibiting chaotic behavior. To address this issue a rigorous proof of chaos is necessary. We will now outline the approach for a rigorous proof of chaos in Chua's attractor.

3.1. *Piecewise-Linear Analysis of Chua's Circuit*

The method employed in[Chua et. al.(1986)] was the very first rigorous proof of chaos in any physical, and not hypothetical, dynamical system. The essence of this approach is Shilnikov's theorem.

Theorem 1. *Let ξ be a continuous piecewise-linear vector field associated with a third-order autonomous system $\dot{\mathbf{x}} = \mathbf{f}(\mathbf{x}), \mathbf{x} \in \Re^3$. Assume the origin is an equilibrium point with a pair of complex conjugate eigenvalues $\sigma \pm j\omega, (\sigma < 0, \omega \neq 0)$ and a real eigenvalue $\gamma > 0$ satisfying $|\sigma| < \gamma$. If in addition, ξ has a homoclinic orbit through the origin, then ξ can be infinitesimally perturbed into a nearby vector field ξ^* with a countable set of horseshoes.*

The difficult part of Shilnikov's theorem is rigorously confirming the existence of a homoclinic orbit at the origin. Such an orbit is double-asymptotic at the origin, that is, $\mathbf{x}_h(t) \to \mathbf{0}$ as $t \to \pm\infty$. However, because of

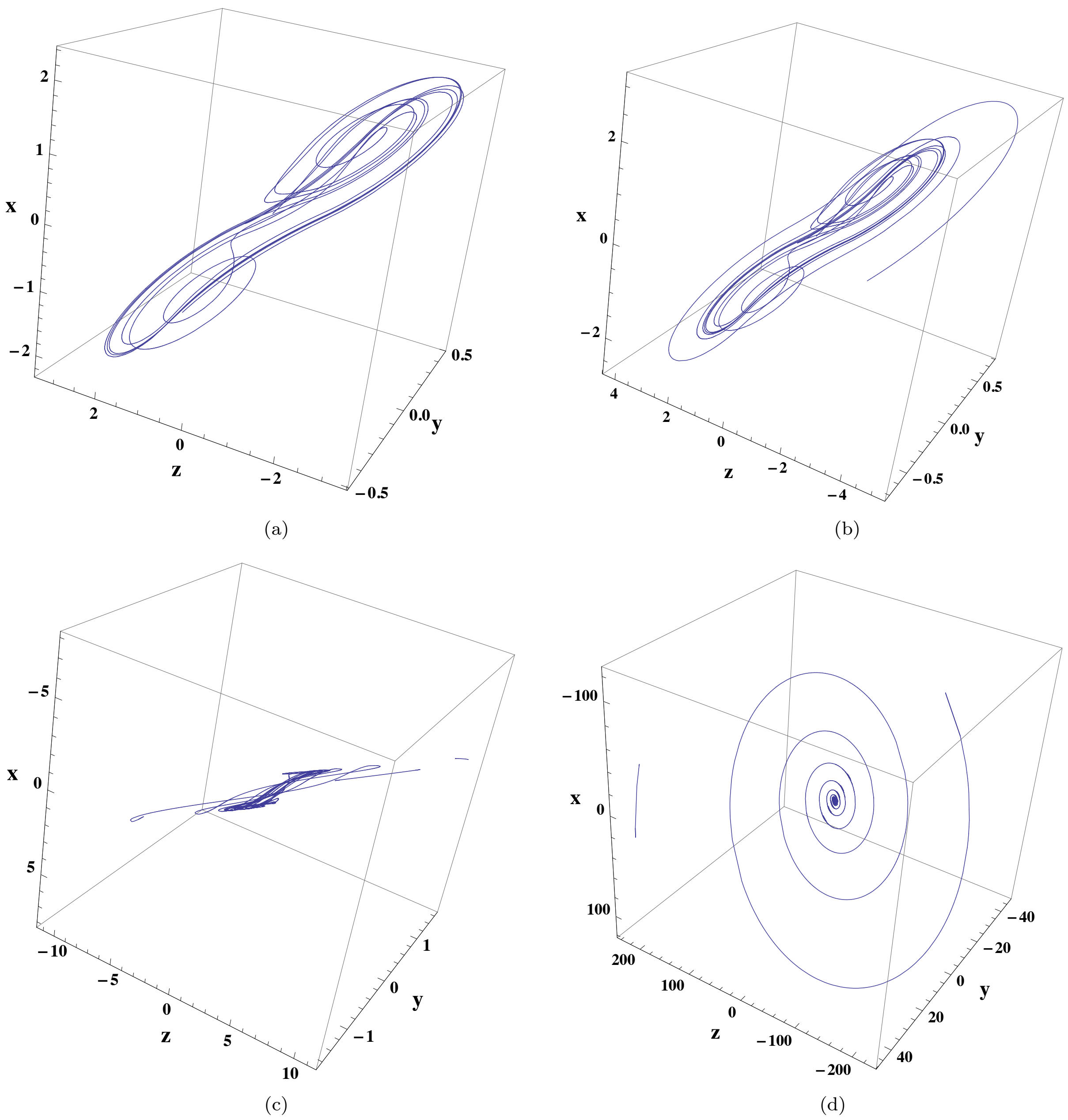

Fig. 9. Trajectory of Chua's circuit with $\alpha = 10.75$: (a) for t = 30 units, (b) for t = 35 units, (c) for t = 45 units and (d) for t = 70 units. Notice how in each case the dimensions of our axes are increasing. The transient attractor is not even visible in (d). In other words Chua's circuit is unstable for this choice of parameter values. In the physical circuit we will quickly observe a large amplitude limit cycle due to amplifier saturation.

the piecewise-linear nature of the nonlinearity, we analyze the system in each linear region and then carefully "stitch" the trajectories at the boundaries. Since closed form solutions of trajectories and eigenspaces can be found for linear systems, we can plot the geometrical structure and typical trajectories of the piecewise-linear system. Fig. 10 shows a typical plot of eigenspaces for Chua's circuit.

The detailed analysis is very involved and the reader is encouraged to go through the double scroll family paper[Chua et. al.(1986)] to understand the complete picture (such as rigorous analysis of bifurcation phenomenon). But there are three essential steps and we have included relevant equation, page numbers from the double

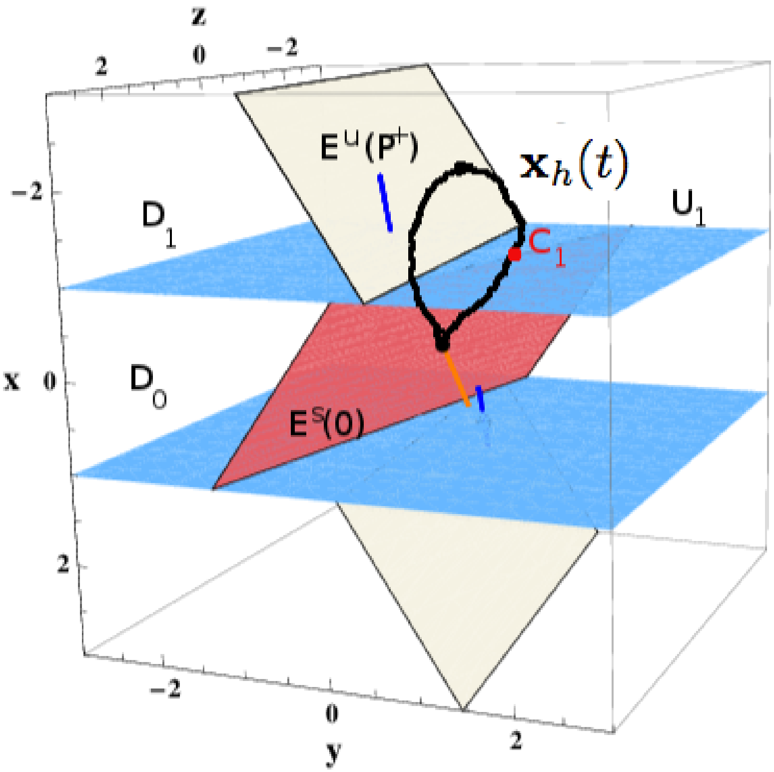

Fig. 10. Eigenspaces for the Chua system. The nonlinearity separates phase space into three distinct regions. $E^s(0)$ is the stable complex eigenspace associated with the origin. $E^u(P^+)$ is the unstable complex eigenspace associated with P^+. For clarity, only the complex eigenspaces are shown. A trajectory $\mathbf{x}_h(t)$ initially starts along the unstable real eigenspace associated with the origin. Once the trajectory passes into D_1, it is shown here to spiral tangentially to $E^u(P^+)$ before going through C_1. If there exists a C_1 such that it also lies on the line of intersection between $E^s(0)$ and U_1, we have found a homoclinic orbit $\mathbf{x}_h(t)$. We have exaggerated the homoclinic orbit by hand for clarity.

scroll family paper[Chua et. al.(1986)] for correlating the "cookbook" approach in this chapter with Chua's original work.

(1) Determine the eigenvalues for each of the linear regions in Chua's system (Eqs.(16) through (19)). The transition matrix for region D_0 is

$$M_0 = \begin{pmatrix} -\alpha m_0 & \alpha & 0 \\ 1 & -1 & 1 \\ 0 & -\beta & 0 \end{pmatrix} \tag{22}$$

The transition matrix for region D_1 is

$$M_1 = \begin{pmatrix} -\alpha m_1 & \alpha & 0 \\ 1 & -1 & 1 \\ 0 & -\beta & 0 \end{pmatrix} \tag{23}$$

Thus the eigenvalues for Eqs.(22) are $\tilde{\gamma}_0, \tilde{\sigma}_0 \pm \tilde{\omega}_0$ and for (23) are $\tilde{\gamma}_1, \tilde{\sigma}_1 \pm \tilde{\omega}_1$.

(2) Define necessary normalized eigenvalues (Eqs. (2.9) and (2.12), p. 1076[Chua et. al.(1986)]) and strategic points (Eqs. (2.20) through (2.33), pp. 1077-1078[Chua et. al.(1986)]).

$$\sigma_{0,1} = \frac{\tilde{\sigma}_{0,1}}{\tilde{\omega}_{0,1}} \qquad \gamma_{0,1} = \frac{\tilde{\gamma}_{0,1}}{\tilde{\omega}_{0,1}} \qquad k_0 = \frac{-\tilde{\gamma}_0}{\tilde{\gamma}_1} \qquad k_1 = \frac{-\tilde{\gamma}_1}{\tilde{\gamma}_0} \tag{24}$$

$$p_0 = \sigma_0 + \frac{k_0}{\gamma_0}\left(\sigma_0^2 + 1\right) \qquad p_1 = \sigma_1 + \frac{k_1}{\gamma_1}\left(\sigma_1^2 + 1\right) \tag{25}$$

$$Q_0 = (\sigma_0 - \gamma_0)^2 + 1 \qquad Q_1 = (\sigma_1 - \gamma_1)^2 + 1 \tag{26}$$

(3) Compute the following quantities and check if the given conditions are satisfied.

$$a_1 = \frac{-\sigma_1\gamma_1(p_1^2 + 1)}{Q_1} > 0 \tag{27}$$

$$\begin{aligned} a_2 = Q_0^2 + \gamma_0^2(1 + p_0^2(2 + (\gamma_0 - \sigma_0)^2) + 2(\gamma_0 - \sigma_0)^2 + 2p_0(\sigma_0 - \gamma_0)) \\ + Q_0\gamma_0(-3\gamma_0 + 3\sigma_0 + p_0(2 + p_0(\sigma_0 - \gamma_0)) > 0 \end{aligned} \tag{28}$$

$$a_3 = \sigma_1\left(1 + \frac{2}{\sigma_1^2 - 1}\right) \geq \gamma_1 \tag{29}$$

$$a_4 = (1 + p_0^2) - (1 + \sigma_0^2)e^{2\sigma_0(\tan^{-1}(p_0) - \tan^{-1}(\sigma_0))} > 0 \tag{30}$$

$$0 < a_5 = (1 + p_0^2)e^{\sigma_0\left(\frac{\pi}{2} - \tan^{-1}(p_0)\right)} < 1 \tag{31}$$

$$\begin{aligned} a6 = \frac{\gamma_1(1 - \sigma_1(\sigma_1 - \gamma_1))}{Q_1} - \frac{(\sigma_1^2 + 1)\gamma_0 k_1}{(\sigma_0^2 + 1)\gamma_1 Q_1} \\ \cdot (k_1\gamma_0(\sigma_1(\sigma_1 - \gamma_1) + 1) + 2\sigma_0\gamma_1(\sigma_1 - \gamma_1)) > 0 \end{aligned} \tag{32}$$

$$0 < a7 = \frac{\sigma_1^2 + 1}{Q_1(\sigma_0^2 + 1)}\gamma_0 k_1(\gamma_0 k_1 - 2\sigma_0) < 1 \tag{33}$$

The conditions in Eqs. (27) through (30) check if the spiral trajectory in D_1 is sandwiched between two logarithmic spirals, for all time t. Thus one can ensure that the trajectory does not enter the stable eigenspace in D_1 (this would destroy the homoclinic orbit). These conditions also ensure that there is no "bouncing" behavior of the trajectory at the boundary U_1 in Fig. 10. Eq.(27) is Eq.(5.27) along with the condition in Eq.(5.24) on p. 1093.[Chua et. al.(1986)] Eq.(28) can be obtained by using Eqs.(2.20) and 2.22) on p.1077[Chua et. al.(1986)] and then imposing the condition $\mathbf{OB_0} \cdot \mathbf{B_0A_0} > 0$. Eq.(29) is Eq.(5.36) on p.1094.[Chua et. al.(1986)] Eq.(30) is derived from Eqs.(5.37) and (5.39) on p.1094,[Chua et. al.(1986)] along with the definition $\tan(\phi + \theta_0) = p_0$. Eq.(31) is to check that once the trajectory re-enters D_0, it does not intersect the plane $x = -1$. Eqs.(32) and (33) are to ensure that the point C_1 in Fig. 10 lies on the stable eigenspace $E^s(0)$ associated with the origin. These two conditions imply orbit $\mathbf{x}_h(t)$ in Fig. 10 does approach the origin as $t \to \infty$. Eq.(31) is obtained from Eqs. (5.48) and (5.49) on p. 1094.[Chua et. al.(1986)] Eq.(32) is obtained by imposing the condition in Eq.(5.56) on Eq.(5.57) (p. 1095[Chua et. al.(1986)]). Eq.(33) is obtained by imposing the condition in Eq.(5.56) on Eq.(5.58) (p. 1095[Chua et. al.(1986)]).

Note that all the expressions in Eqs. (27) through (33) are in closed form and hence we can calculate the result to the required precision. Also, the equations hold for corresponding trajectories from D_0 to D_{-1}.

We will now apply the technique to both prove and disprove chaos in Chua's circuit. In other words, one needs to be very careful in choosing the correct parameter values required for chaos. Not all parameter values for a dynamical system lead to chaotic behavior. Before we begin, note for both proofs below, the detailed calculations from Mathematica 8 (in the form of a pdf file) are available online at `http://myweb.msoe.edu/muthuswamy/MuthuswamyWSPC2011ChuaBook-OnlineFiles/`.

First we will prove that Chua's circuit is chaotic for parameter values $\{\alpha, \beta, m_0, m_1\} = \{9, 14\frac{2}{7}, -1/7, 2/7\}$.

Proof. Step one is to determine if the origin is an equilibrium point and is a hyperbolic saddle under Jacobi linearization. For our parameter values, the origin is an equilibrium point and the eigenvalues of linearized system at the origin are $\tilde{\gamma}_0 \approx 2.22, \tilde{\sigma}_0 \pm j\tilde{\omega}_0 \approx -0.97 \pm j2.71$. Thus Shilnikov's first condition is satisfied.

Now, we prove that there exists a homoclinic orbit based at the origin. One can compute and verify that all conditions in step (3) from the previous section are satisfied. Hence, there exists a homoclinic orbit at the origin.

□

Now we will prove that Chua's circuit is not chaotic for parameter values $\{\alpha, \beta, m_0, m_1\} = \{10.75, 14\frac{2}{7}, -1/7, 2/7\}$. We only changed the α parameter.

Proof. Step one is to determine if the origin is an equilibrium point and is a hyperbolic saddle under Jacobi linearization. For our parameter values, the origin is an equilibrium point and the eigenvalues of linearized system at the origin are $\tilde{\gamma}_0 \approx 2.73, \tilde{\sigma}_0 \pm j\tilde{\omega}_0 \approx -1.10 \pm j2.61$. Thus Shilnikov's first condition is satisfied.

However we can determine that the last condition in step (3), Eq.(33), is not satisfied. In other words, there exists some $t > 0$ for which the point C_1 from Fig. 10 does not lie on the stable eigenspace associated with the origin. Note that we cannot determine t, we just know that a homoclinic orbit cannot exist for the given set of parameter values.

□

Notice that our results for the value of $\alpha = 10.75$ agree with published[Chua et. al.(1986)] results on the "death of the Double-Scroll".

The piecewise-linear analysis technique in this section is especially useful since it can be applied to other chaotic systems via the Global Unfolding Theorem. A short tutorial on this important theorem is the topic of the next section.

4. The Global Unfolding Theorem

The piecewise-linear analysis technique from the previous section can be used to "globally unfold" Chua's circuit such that the resulting dynamical system is imbued with every possible qualitative dynamics of an extremely large family $\mathcal{C}$ of piecewise-linear dynamical systems.[Chua(1992)] This unfolding of Chua's circuit is obtained by simply adding a resistor R_0 in series with inductor L and is shown in Fig. 11. This new circuit is called Chua's oscillator.

In this section, we provide a short tutorial on the global unfolding theorem. First, the algorithm for global unfolding is shown below.

(1) Confirm that the system in question belongs to family $\mathcal{C}$.[Chua(1992)] That is, the system defined by state equation

$$\dot{\mathbf{x}} = \mathbf{f}(\mathbf{x}), \mathbf{x} \in \Re^3 \tag{34}$$

has the following properties:

  (1) $\mathbf{f}(\cdot)$ is continuous
  (2) $\mathbf{f}(\cdot)$ is odd-symmetric (could also be with respect to a point other than the origin)
  (3) $\Re^3$ is partitioned by 2 parallel boundary planes U_1 and U_{-1} into an inner region D_0 containing the origin and two outer regions D_1 and D_{-1}.

(2) Let (μ_1, μ_2, μ_3) and (ν_1, ν_2, ν_3) be the eigenvalues associated with the linear (D_0 region) and affine ($D_{1,-1}$ regions) respectively.

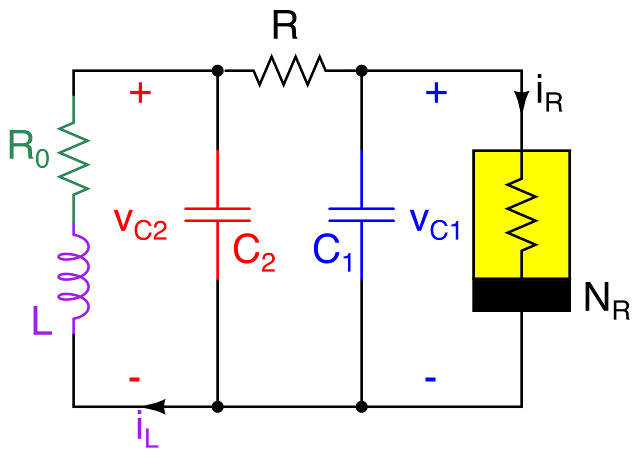

Fig. 11. Chua's oscillator obtained from Chua's circuit by adding linear passive resistor R_0. Note that R_0 is not the parasitic resistance associated with the inductor.

(3) Compute the equivalent eigenvalue parameters for Chua's oscillator from the following expressions. If $p_1 = q_1$, slightly perturb p_1 and q_1 : $p_1 = p_1 + \delta, q_1 = q_1 - \delta$.[Chua(1992)]

$$p_1 = \mu_1 + \mu_2 + \mu_3 \qquad q_1 = \nu_1 + \nu_2 + \nu_3 \tag{35}$$

$$p_2 = \mu_1\mu_2 + \mu_2\mu_3 + \mu_3\mu_1 \qquad q_2 = \nu_1\nu_2 + \nu_2\nu_3 + \nu_3\nu_1 \tag{36}$$

$$p_3 = \mu_1\mu_2\mu_3 \qquad q_3 = \nu_1\nu_2\nu_3 \tag{37}$$

(4) Compute the equivalent circuit parameters for Chua's oscillator from the following expressions.[Chua(1992)]

$$k_1 \triangleq -p_3 + \frac{q_3 - p_3}{q_1 - p_1}\left(p_1 + \frac{p_2 - q_2}{q_1 - p_1}\right) \tag{38}$$

$$k_2 \triangleq p_2 - \left(\frac{q_3 - p_3}{q_1 - p_1}\right) + \left(\frac{p_2 - q_2}{q_1 - p_1}\right)\left(\frac{p_2 - q_2}{q_1 - p_1} + p_1\right) \tag{39}$$

$$k_3 \triangleq \left(\frac{p_2 - q_2}{q_1 - p_1}\right) - \frac{k_1}{k_2} \tag{40}$$

$$k_4 \triangleq -k_1k_3 + k_2\left(\frac{p_3 - q_3}{p_1 - q_1}\right) \tag{41}$$

$$C_1 = 1 \tag{42}$$

$$C_2 = -\frac{k_2}{k_3^2} \tag{43}$$

$$L = -\frac{k_3^2}{k_4} \tag{44}$$

$$R = -\frac{k_3}{k_2} \tag{45}$$

$$R_0 = -\frac{k_1k_3^2}{k_2k_4} \tag{46}$$

$$G_a = -p_1 - k_3 - \frac{k_1}{k_2} + \frac{k_2}{k_3} \tag{47}$$

$$G_b = -q_1 - k_3 - \frac{k_1}{k_2} + \frac{k_2}{k_3} \tag{48}$$

We will now apply the algorithm above to the system from[Nishio et. al. (1992)] and thus obtain an attractor from Chua's circuit that is topologically conjugate to the attractor from.[Nishio et. al. (1992)]

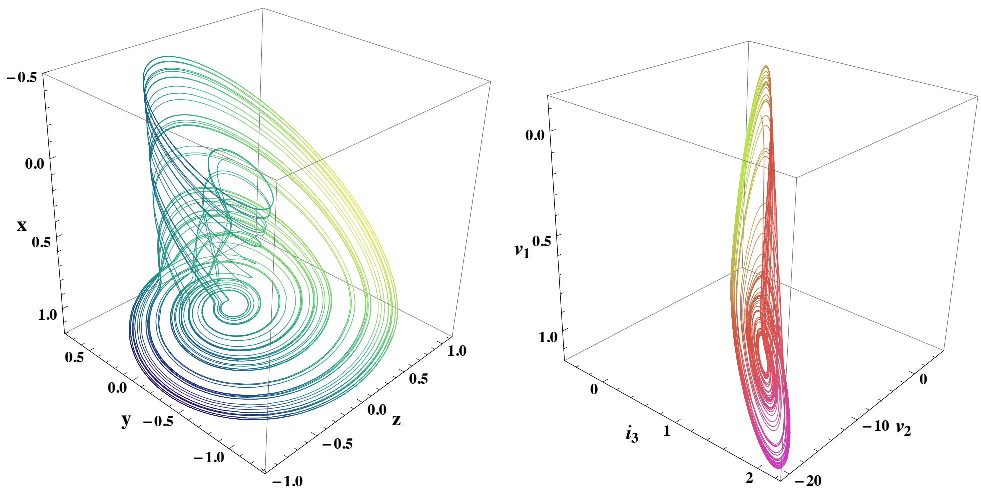

(a) (b)

Fig. 12. (a) is the original system from.Nishio et. al. (1992) Parameter values for simulation are $a = 0.35, b = 1, \alpha = 0.5, \epsilon = 0.1$, initial conditions are $(0.1, 0.1, 0.1)$. (b) shows the linearly conjugate attractor for Chua's oscillator.

(1) The system of equations for the nonlinear inductor circuit is given by Eqs.(49) through (52).

$$\dot{x} = -bz - bf(x) \tag{49}$$

$$\dot{y} = z \tag{50}$$

$$\dot{z} = (a-b)z - y - bf(x) \tag{51}$$

$$f(x) = \frac{x}{\epsilon} - \left(\alpha + \frac{1}{\epsilon}\right)\frac{|x+1| - |x+1|}{2} \tag{52}$$

Note that our system satisfies the conditions in step 1. Hence it can be mapped into Chua's oscillator.

(2) (μ_1, μ_2, μ_3) and (ν_1, ν_2, ν_3) are computed to be $(0.367, -0.283+1.131i, -0.283-1.31i)$ and $(-10.967, -0.133+0.946i, -0.133-0.946i)$.

(3) $(p_1, p_2, p_3, q_1, q_2, q_3)$ are computed to be $(-0.2, 1.15, 0.499, -10.7, -2, -10)$.

(4) Equivalent circuit parameters are thus $C_1 = 1, C_2 = -0.0326, L = -2.76, R = -10.116, R_0 = 9.2055, G_a = 0.5989, G_b = 11.099$.

Figure 12 shows the results. Notice how the attractor from Chua's oscillator is a linear transformation of the original attractor from.Nishio et. al. (1992) Once we have globally unfolded a dynamical system into Chua's oscillator, we can apply the piecewise-linear analysis technique from the previous section to rigorously prove the existence of chaos.

5. Conclusions

From the date of invention and realization of Chua's circuit, it took two years to publish a rigorous proof of chaos. In this chapter, we covered all the main ideas from this time period. This chapter has thus provided the reader with all the tools necessary for further study of chaos in piecewise-linear dynamical systems. Ever since Chua's seminal work, a variety of other chaotic circuits have been discovered. Sprott's "jerky dynamics" based chaotic circuitsSprott(2000) are especially elegant. Other techniques for rigorous analysis of chaos also exist, such as ones involving topological horseshoe theory.Yang (2009)

For future work, a particularly interesting concept to explore is the minimal number of circuit elements required for chaos. Referring to Chua's circuit in Fig. 3, one can ask if we can eliminate the linear resistor R. This would however reduce the number of states from three to two since capacitors C_1 and C_2 are now in

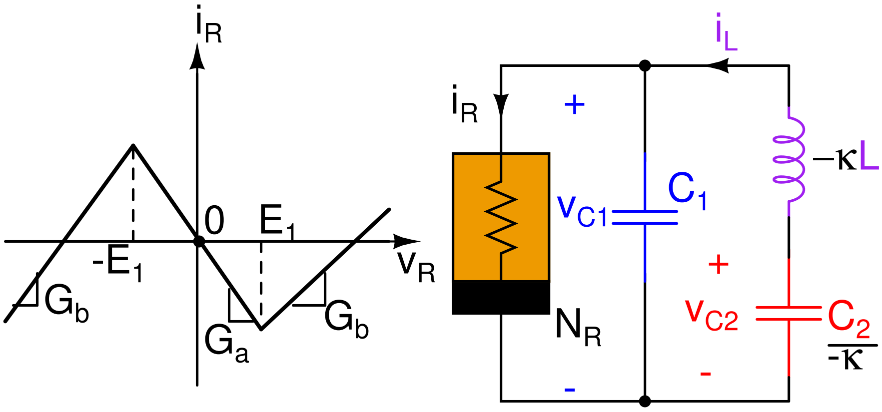

Fig. 13. The Four-Element Chua's circuit. The nonlinear resistor N_R has only one region of negative slope. Note that in the circuit $v_{C1} = v_R$. Capacitor C_2, C_1 and inductor L_1 are linear passive elements. C_2 and L_1 are made active $(-\kappa, \kappa > 0)$ using an operational amplifier that acts as a current inverter.

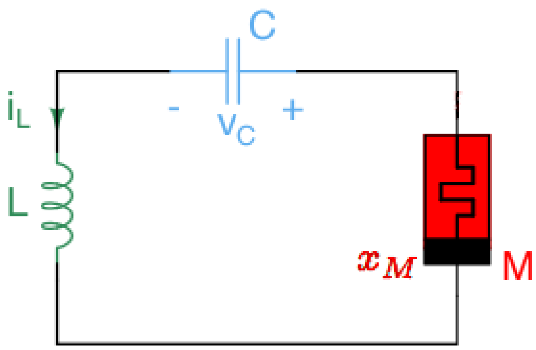

Fig. 14. The three element chaotic circuit. This circuit is simplest in the sense that we have only three elements and each element contributes to one of the three states required for chaos. Also the only nonlinear active element is the memristor, the capacitor and inductor are linear passive elements. Internal state of the memristor is denoted by x_M. The physical interpretation of this internal state depends on the memristor used.

parallel. But in 2008, 25 years after the invention of Chua's circuit, Barboza and Chua reduced the number of elements by re-arranging Chua's circuit as shown in Fig. 13.[Barboza and Chua(2008)] Note that in reality, the nonlinear resistor in Fig. 13 has only one region with negative slope. The original Chua's circuit had three regions with negative slope. Nevertheless, Barboza and Chua demonstrated the circuit in Fig. 13 is linearly conjugate to Chua's circuit.

Muthuswamy and Chua further eliminated the number of elements required for chaos by one when they systematically designed the circuit in Fig. 14.[Muthuswamy and Chua(2010)] However the nonlinear characteristics of the memristor do not resemble the piecewise-linear nonlinearity in Chua's circuit. Thus a good candidate for future research would be to design a memristor with piecewise-linear characteristics to answer the question : does the three element circuit have a chaotic attractor that is topologically conjugate to the double scroll?

Acknowledgments

The author would like to thank Dr. Jean-Marc Ginoux, Dr. Jovan Jevtic and Dr. Gerald Thomas for insightful comments.

References

Alligood et. al.(1996). Alligood, K. T., Sauer, T. D. and Yorke J. A. (1996). *Chaos : An Introduction to Dynamical Systems* (Springer).

Barboza and Chua(2008). Barboza, R. and Chua, L. O. (2008). ”The Four-Element Chua’s Circuit”, *International Journal of Bifurcation and Chaos*, Vol. 18(4). pp. 943-955.

Brown and Chua(1996). Brown, R. and Chua, L. O. (1996). ”Clarifying Chaos : Examples and Counterexamples”, *International Journal of Bifurcation and Chaos*, Vol. 6(2). pp. 219-249.

Chua et. al.(1986). Chua, L. O., Kumoro, M. and Matsumoto, T. (1986). ”The Double Scroll Family”, *IEEE Transactions on Circuits and Systems*, Vol. 33(11). pp. 1072–1118.

Chua(1992). Chua, L. O. (1992). ”The Genesis of Chua’s Circuit”, *Archiv fur Elektronik und Uebertragungstechnik*, Vol. 46(4). pp. 250–257.

Chua(1993). Chua, L. O. (1993). ”Global Unfolding of Chua’s Circuit”, *IEICE Transactions on Fundamentals of Electronics, Communications and Computer Sciences*, Vol. E76-A(5). pp. 704–734.

Kennedy(1992). Kennedy, M. P. (1992). ”Robust OP Amp Realization of Chua’s Circuit”, *Frequenz*, Vol. 46(3-4), pp. 66–80.

Lorenz(1963). Lorenz, E. N. (1963). ”Deterministic Nonperiodic Flow”, *Journal of Atmospheric Sciences*, Vol. 20, pp. 130–141.

Matsumoto(1984). Matsumoto, T. (1984). ”A Chaotic Attractor from Chua’s Circuit”, *IEEE Transactions on Circuits and Systems*, Vol. 31(12). pp. 1055–1058.

Matsumoto et. al.(1985). Matsumoto, T., Chua, L. O. and Komuro, T. (1985). ”The Double Scroll”, *IEEE Transactions on Circuits and Systems*, Vol. 32(8). pp. 797–818.

Muthuswamy and Chua(2010). Muthuswamy, B. and Chua, L. O. (2010). ”Simplest Chaotic Circuit”, *International Journal of Bifurcation and Chaos*, Vol. 20(5). pp. 1567–1580.

Nishio et. al. (1992). Nishio, Y., Mori, S. and Inaba, N. (1992). ”Chaotic Phenomena In an Autonomous Circuit with a Nonlinear Negative Inductor”, *Electronics and Communication in Japan*, Vol. 75(12). pp. 72-81.

O’Donoghue et. al. (2005). O’Donoghue, K., Kennedy, M. P., Forbes, P., Qu, M. and Jones, S. (2005). ”A Fast and Simple Implementation of Chua’s Oscillator with Cubic-Like Nonlinearity”, *International Journal of Bifurcation and Chaos*, Vol. 15(9), pp. 2959-2971.

Rossler(1976). Rössler, O. E. (1976). ”An Equation for Continuous Chaos”, *Physics Letters*, 57A(5). pp. 397–398.

Sprott(2000). Sprott, J. C. (2000). ”Simple chaotic systems and circuits”, *American Journal of Physics*, 68(8), pp. 758-763.

Tokunaga et. al.(1989). Tokunaga, R., Komuro, M., Matsumoto T. and Chua, L. O. (1989). ”’Lorenz Attractor’ from an Electrical Circuit with Uncoupled Continuous Piecewise-Linear Resistor”, *International Journal of Circuit Theory and Applications*, Vol. 17(1). pp. 71–85.

Tucker(1999). Tucker, W. (1999). *The Lorenz Attractor Exists*, Available from : <`http://www2.math.uu.se/~warwick/main/thesis_2.1.html`>. [13 November 2011].

Mathematica(2011). Wolfram Research. (2011). *Wolfram Research - Mathematica 8*. Available from : <`http://www.wolfram.com`>. [13 November 2011].

Yang (2009). Yang, X. S. (2009). ”Topological Horseshoes and Computer Assisted Verification of Chaotic Dynamics”, *International Journal of Bifurcation and Chaos*, Vol. 19(4). pp. 1127–1145.